Applied Chemical Engineering (2025) Volume 9 Issue 2 ISSN: 2578-2010 (O)
doi: 10.59429/ace.v9i2.5863

RESEARCH ARTICLE

Evaluation of Methanolic Extract of Inula graveolens L. as Antioxidant and Corrosion Inhibitor for Carbon Steel Alloy using MATLAB

Khawlah S. Burghal[1*], Hind Abdel Amier Sabti[2], Adnan Jassim Mohammed Al-Fartosy[3]

[123] *Department of Chemistry, College of Science, University of Basrah, 61004 Basrah, Iraq*

***Corresponding author:** Khawlah S. Burghal, khawla.brqaal@uobasrah.edu.iq

ABSTRACT

In recent years, Antioxidants have played a crucial role in various applications, and their potential has been evaluated through multiple assays Antioxidant utilizing 2, 2-diphenyl-1-picryl-hydrazyl-hydrate (DPPH), β-carotene assay and environmentally friendly corrosion resistance property for alloy carbon steel in 1M HCl was investigated in both in the absence and presence of methanolic extract of Inula graveolens L (MEIG). Using the Tafel Plot method, the impact of temperature and inhibitor concentration was studied MEIG gave good antioxidant activity, including β-carotene (83%) and DPPH (73.9%), and exhibited a maximal (99.5%) inhibitory efficiency at 323 k. Kinetic parameters (Ea, ΔG*, ΔS*and ΔH*,) were calculated. MEIG increased the energy barrier of the corrosion reaction, making it non-spontaneous through an endothermic mechanism. Furthermore, ΔHads, ΔGads, and ΔSads were also calculated, demonstrating that the inhibitor was physically adsorbed via a spontaneous. However, inhibition efficiency decreased with rising temperature due to weakened adsorption and desorption effect Simply blocking the reaction sites inhibited the corrosion. The absorption process sold the Langmuir equation for heat absorption. The study highlights MEIG's dual functionality as a potent antioxidant and an effective, environmentally friendly corrosion inhibitor models was processed using MATLAB computer programming.

Keywords: Inula graveolens L., antioxidants, corrosion inhibitors, acidic corrosive media, carbon steel alloy

ARTICLE INFO

Received: 19 December 2025
Accepted: 03 March 2026
Available online: 14 April 2026

Introduction

Oxidation is a significant problem in various fields such as human health and food production. It also affects industrial areas, causing corrosion in metal containers and structures, leading to economic losses and reduced product quality. [1-3] Creating metal implants that are resistant to corrosion is a challenging endeavor, especially in the field of biomedical engineering. If corrosion were to occur after implantation in the human body, it could pose serious risks. [4] Researchers worldwide often cite this as a key reason for seeking effective corrosion inhibitors. These inhibitors can be natural, semi-synthetic, or synthetic, and are chosen based on specific requirements[5].

As a result, investigating corrosion mitigation strategies is necessary. As a sustainable and eco-friendly substitute, green corrosion inhibitors derived from organic materials such as plant extracts have been created. There is a constant push to discover potent, naturally derived corrosion inhibitors. [6,7] Corrosion-resistant materials are commonly found in industries that operate in corrosive environments, such as food processing and marine applications (e.g., ships). Creating

metal implants that are resistant to corrosion is a challenging endeavor, especially in the field of biomedical engineering. If corrosion were to occur after implantation in the human body, it could pose serious risks.[8-10] Researchers worldwide often cite this as a key reason for seeking effective corrosion inhibitors. These inhibitors can be natural, semi-synthetic, or synthetic, and are chosen based on specific requirements. There is a constant push to discover potent, naturally derived corrosion inhibitors. [11,12] Examples of these active substances include pectin, amino acids, alkaloids, polyphenols, and fatty acids derived from plants[13].

However, some chemicals' toxicity has restricted the use of organic compounds. The use of plant extracts as efficient corrosion inhibitors that don't affect the environment is currently popular. These inhibitors also offer a number of benefits, like as affordability, ease of manufacture, and availability, which promote their use as substitutes for chemically produced molecules.[14]

According to a number of studies, using an alcoholic or aqueous plant extract can effectively lessen the corrosion of active metals in various mediums.

Research has shown that green inhibitors, such as flavonoids, play a crucial role in preventing corrosion. [15,16] In folk Iraqi medicine, Inula graveolens L. is used to treat various ailments such as rheumatic fever, convulsions in babies, toothaches, high blood sugar, dissolving internal blood clots, and aiding digestion.[17]

In this study, we investigated the potential of Inula graveolens L. methanolic extract as a natural antioxidant and corrosion inhibitor for carbon steel in acidic environments at varying temperatures .

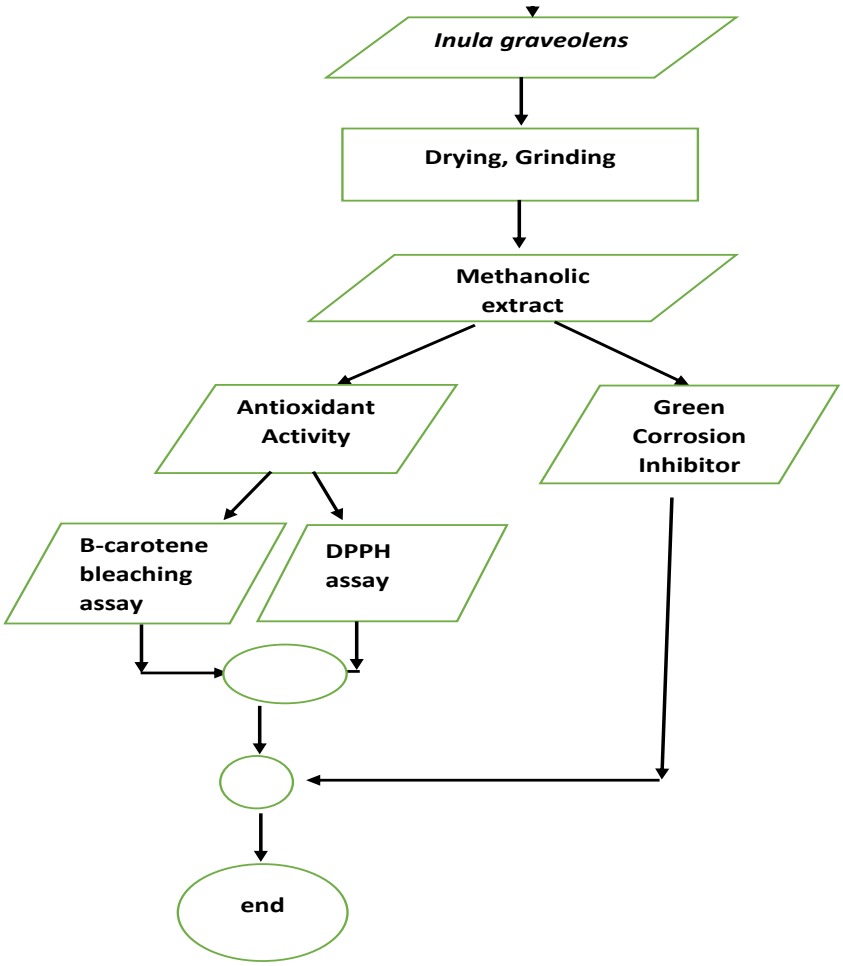

Figure 1. Aworkflow diagram for predicting the effectiveness of extracts as antioxidants and corrosion inhibitors using the MATLAB graphical user interface. The process begins with user-defined inputs, such as plant treatment, effectiveness measurement, and corrosion analysis.

Experimental

1. Plant material

1.1. Plant collection and identification

The plant Inula graveolens L. used in this study was collected in October 2022 from the Abu-Al-Khaseeb district in Iraq, south of Basra. The plant was botanically authenticated, and voucher specimens were deposited in the Herbarium of Basrah

(Iraq, Basrah, College of Science, University of Basrah).

1.2. Extraction procedure

100 g of powdered plant material was extracted with 80% methanol in a Soxhlet extractor for 24 h. The methanol extract (MEIG) was filtered and then dried under reduced pressure in a rotary evaporator. [18] The yield of dry extract was 9.47 g.

2. Antioxidant activity assays

2.1. DPPH free radical-scavenging assay

The assay was used to measure the spectrophotometric capacity to scavenge free radicals. In summary, 160 µL of DPPH (0.1 mM) and 40 µL of MEIG at 00 ppm of concentration were mixed together. The combination changed into vigorously shaken for 30 minutes, and the residual DPPH, Absorbance at 517 nm was measured. For comparison, standard antioxidant was used as a BHT. The DPPH radical scavenging capacity was determined using the formula Equation 1.

$$\text{DPPH (scavenging) effect (\%)} = \frac{A_{\text{control}} - A_{\text{sample}}}{A_{\text{control}}} \times 100 \quad (1)$$

2.2. β-Carotene/linoleic acid assay

Using the system β-carotene-linoleic acid as stated, the β-carotene bleaching activity was evaluated. 0.2 g of Tween 20,20 mg of linoleic acid, and 2 mg of β-carotene in 10 ml of chloroform were combined to create the solution. Distilled water 50mL was added of aerated to the flask while shaking after the chloroform was extracted using a rotary evaporator set to 30 °C under vacuum to 30 °C under vacuum. Aliquots (5 mL) of the emulsion were placed in tubes with 0.2 mL of the extract (MEIG, 50 and 100 ppm) or the reference substance Butylated hydroxytoluene (BHT, 50 and 100 g L^{-1}). 0.2 mL of 80% methanol was present in the control. The emulsion as soon as was added, the absorbance at 470 nm was measured. After that, the samples were heated to 50 °C for thermal autoxidation, and absorbance readings were taken every 15 minutes until the control sample's β-carotene hue vanished (105 minutes). The rate of extract degradation was reaction kinetics based determined on zero-order. The antioxidant activity (AA) was calculated by comparing the percentage of inhibition to the control Equation 2. [19]

$$\left[1 - \frac{A_i - A_t}{A_i^0 - A_t^0}\right] \times 100 \quad (2)$$

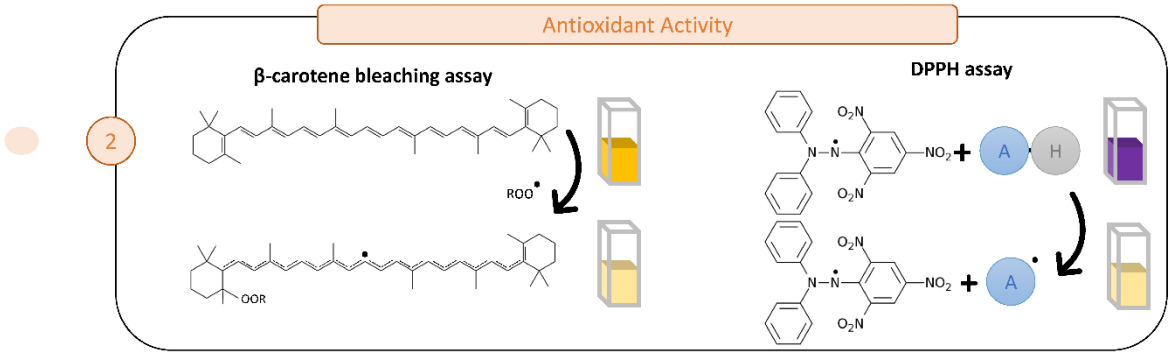

Figure 1. Antioxidant Activity assays for DPPH free radical-scavenging assay, β-Carotene/linoleic acid assay.

3. Corrosion study

The inclusion of flavonoids as corrosion inhibitors for C1010 carbon steel alloys was evaluated in this study using Tafel plot method

3.1. The Composition of Alloys

In this study, we used a carbon steel alloy (C1010) measuring 3 cm in length, 1.24 cm in breadth, and 0.14 cm in thickness. The alloy comprised of standard strips received from Metal Samples U.S.A. in Alabama, with the composition specified in Table 1. The total immersed strip area was 8.45 cm2.

Table 1 lists the carbon steel alloy C1010's chemical composition as a percentage of weight.

Table 1. Elements Composition of Carbon Steel Alloy (C1010)

Elements	C	P	Ni	S	Mn	Cr	Si	As	Cu	Fe
% w/w	0.13	0.04	0.30	0.05	0.30	0.10	0.37	0.08	0.30	Balance

Where: C = Carbon, P = Phosphorus, Ni = Nickel, S = Sulfur, Mn = Manganese, Cr = Chromium, Si = Silicon, As = Arsenic, Cu = Copper, Fe = Iron.

3.2. Preparing the carbon steel samples

The grinding process was carried out using silicon carbide paper with different fineness (100, 120, 200, 400, 600, 1000, and 1200). The samples were cleaned with distilled water and ethanol to remove dirt and iron rust. Subsequently, the samples were polished on a turntable with a soft cloth and alumina to eliminate scratches. After polishing, the samples were cleaned with distilled water and immersed in acetone for approximately 15 minutes. Finally, the samples were dried in desiccators containing silica gel to keep them dry. [20]

3.3. The Electrochemical Cells

This research serves an electrochemical test cell. The cell consists of a 50-mL vessel containing three electrodes: a carbon steel sample for the working electrode, silver in AgCl solution for the reference electrode, and platinum for the counter electrode.

3.4. Experimental Procedure for Tafel Plot Method

The Tafel experiment setup. To calculate corrosion rates, an electric potential vs. current density measurement was conducted using a potentiostat. The potentiostat utilizes various measurement techniques such as Tafel plots, potentiodynamic polarization scans, and linear polarization scans. MEIG inhibitors were prepared at concentrations of 5, 10, and 20 ppm at temperatures of 298, 308, and 328 K in a corrosive environment of 0.1N HCl. [21]

4. Results and discussion

4.1. Antioxidant capacity

The substance that can handle any oxidative damage brought on by free radicals in the body is an antioxidant. UV-V is spectroscopy was used to evaluate the antioxidant activity of the sample at a wavelength of 517 nm, which is the maximum wavelength of DPPH at a concentration of 0.01 mg mL^{-1}. [22-24]

In the presence of antioxidant activity, the sample will cause the DPPH solution's color to change from violet will transition to pale yellow color. The results clearly indicated that the extracts 0.001 inhibited free radicals generation based on concentrations. The DPPH scavenging activity of methanolic extracts of accessions is shown in Table 2. is shown scavenging activity of methanolic extracts of accessions. The highest DPPH radical scavenging activity in methanol extract was noted as 0.001µmol. The antioxidant capacities in DPPH• method, extracts demonstrated 310 the higher inhibition values (except standard) ranged from 73.9%.

Table 2. Scavenging Activity of Methanolic Extracts on DPPH

Compound	Concentration (µg.ml^{-1})	Absorbance at 517nm	Scavenging activity on DPPH (%)
Methanol 80%	100	0.042	73.9

DPPH: 2,2-diphenyl-1-picrylhydrazyl; BHT: Butylated hydroxytoluene (standard).

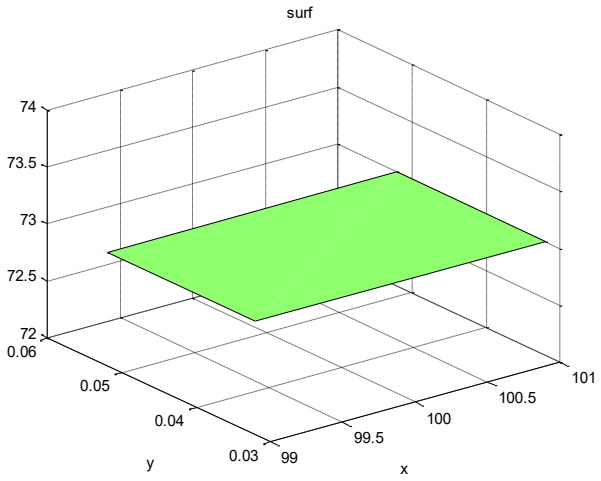

Figure 1. Scavenging Activity of Methanolic Extracts on DPPH by MATLAB

The inhibition of lipid oxidation or free radical scavenging the β-carotene/linoleic acid method is utilized to assess. It was observed that methanolic extraction inhibits the oxidation of linoleic acid, while other extracts are not as effective, as shown in figure 1. Methanolic extraction exhibits antioxidant activity on linoleic acid, with inhibition rates ranging from 83% to high levels compared to BHT (Butylated hydroxytoluene), which is known to inhibit linoleic acid oxidation by 90%.

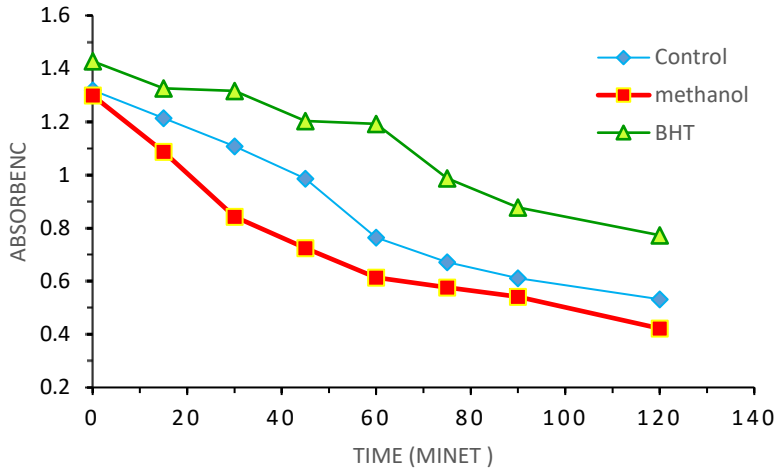

Figure 2. Antioxidant activity of MEIG in β-carotene/linoleic acid assay versus BHT (standard).

4.2. Statistical analysis

Statistical analysis was performed using SPSS software, version 21. The results were expressed as mean ±standard deviation (SD). $p<0.05$ was considered as statistically significant. A p value <0.05 was to be considered statistically significant and $p < 0.01$ for highly significant.

4.3. Electrochemical impedance spectroscopy

Different amounts of methanol extracts were used to study the anodic and cathodic electrochemical polarization. Calculate the corrosion coefficients in the temperature range (228-323) Kelvin which were obtained from the polarization curves and recorded and listed in Table (3). Values of cathodic Tafel slopes (βc), anodic Tafel slopes (βa), corrosion potential (ECorr), corrosion current density (iCorr) and polarization resistance (Rp). Corrosion inhibitors work by preventing corrosion through various mechanisms, depending on their key ingredients. Plant-based green inhibitors function by adsorbing onto the steel surface through physisorption and/or chemisorption. [25]

To prevent corrosion, various plant extracts are extracted and used in complex phytochemical formulations. Plant parts (leaves, bark, stem, fruits, etc.) inhibit corrosion in a specific manner. The essential components determine the precise process underlying corrosion inhibition. Consequently, the primary phytochemical present in a given plant extract can be used to classify and explain the corrosion inhibition process using plant inhibitors[26]. Ionic interactions between charged corrosion inhibitors on the metal surface cause adsorption, reducing the number of active sites. Through the exchange of electrons, the chemical process creates bonds between the metal surface and high-density heteroatoms such as nitrogen, phosphorus, sulfur, and oxygen in the aromatic ring. Inhibition is significantly influenced by the bond strength, the affinity of the aromatic ring, and the carbon chain length, which influence the affinity. The primary component in the plant extract is mostly adsorbed to the steel surface by chemisorption or physical adsorption. [27-28]

Through electrostatic interaction, these inhibitors' positively charged species can physically adsorb onto the metal surface. Benzene rings and oxygen atoms are present in the inhibitor compounds allows for the formation of chemical bonds with the steel surface. Other organic components in addition, the extracts have the ability to adhere to the steel surface.

Studies have shown Figure 3.**a,b** and **c** MEIG (10–20 ppm) at 298–323 K. that the inhibitor performance increases with temperature, with performance improving from 69% at 298 K to 89% at 323 K. The adsorption of these extracts the Langmuir absorption curve is followed through the metal surface.

Tafel polarization curves (Figure 3) demonstrate MEIG's dose-dependent inhibition (69.8–85.1% at 298–323 K).

In Table 3 the calculated values through Tafel extrapolation are shown: current density (Icorr), anodic slope (βa), corrosion rate (Vcorr), corrosion potential (Ecorr) and cathodic slope (βc) and. Current density and corrosion rate are seen to decline as efficiency rises with increasing inhibitor concentration, reaching a maximum efficiency of 98% for methanol extracts.

Tables 3 below show the electrochemical data obtained by the Tafel method, such as corrosion rate (CR) in mpy, corrosion current density (ICorr) in μA.Cm²-, charge transfer resistance (R) in Ω, corrosion potential (ECorr) in mV, and anodic and cathodic Tafel constants (βa and βc) in mV.decade-1, where (decade) means decade of current. The surface coverage area Θ

Table 3. The electrochemical data that acquired by Tafel method for carbon steel alloy(C1010) in absence and presence of methanolic extracts as corrosion inhibitor at (5-20) ppm against corrosive medium of 1M of HCl at (298-328) k

HCl ml	CR (mpy)	R (Ω)	$I_o$corr (μA·cm⁻²)	$E_o$corr (mV)	βc (mV·dec⁻¹)	βa (mV·dec⁻¹)	Θ	%IE
HCl (25)	726.65	17.897	100.58	-0.6101	211.41	190.85		
10	219.6	37.95	474.22	-0.50128	64.431	72.74	0.6977	69.77
15	164.37	50.71	354.96	-0.53622	38.76	38.16	0.7737	77.37
20	108.12	77.09	233.48	-0.5082	80.418	84.69	0.8512	85.12
HCl (35)	806.05	20.56	875.41	-0.5367				
10	113.68	73.326	245.48	-0.5096	105.45	38.936	0.8589	85.89
15	110.95	75.129	239.95	-0.5024	151.15	36.702	0.8623	86.23
20	8.142	1023.7	170.58	-0.5200	18.162	19.677	0.9898	98.98
HCl (50)	1266.1	6.53	2734.2	-549	111.03	46.51		
10	129.2	64.518	278.99	-0.5245	61.171	60.754	0.8979	89.79
15	11.12	19.039	954.45	-0.5168	42.902	43.535	0.9139	91.39
20	5.77	36.641	491.25	-0.5337	55.917	56.37	0.9954	99.54

Where: CR = corrosion rate; R = polarization resistance; $I_o$corr = corrosion current density; $E_o$corr = corrosion potential; βa/βc = anodic/cathodic Tafel slopes; Θ = surface coverage; %IE = inhibition efficiency.

(a)

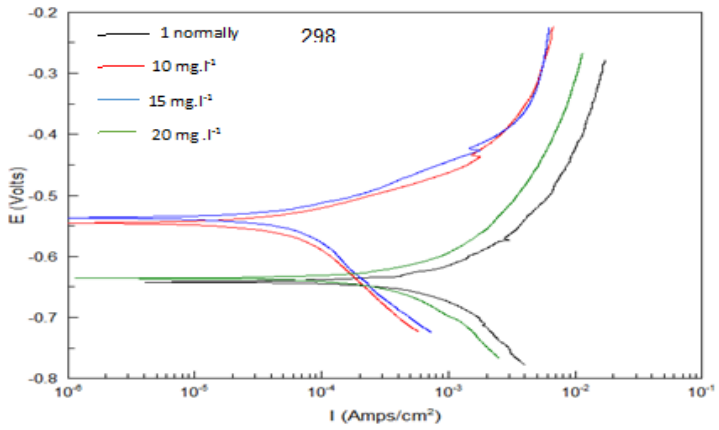

Figure 3a. Tafel plots for carbon steel (C1010) in 1M HCl with MEIG (10–20 ppm) at 298 K

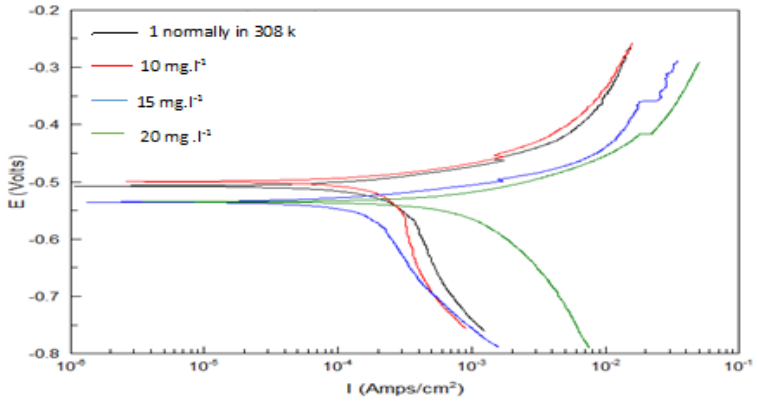

Figure 3. Tafel plots for carbon steel (C1010) in 1M HCl with MEIG (10–20 ppm) at 308 K(b)

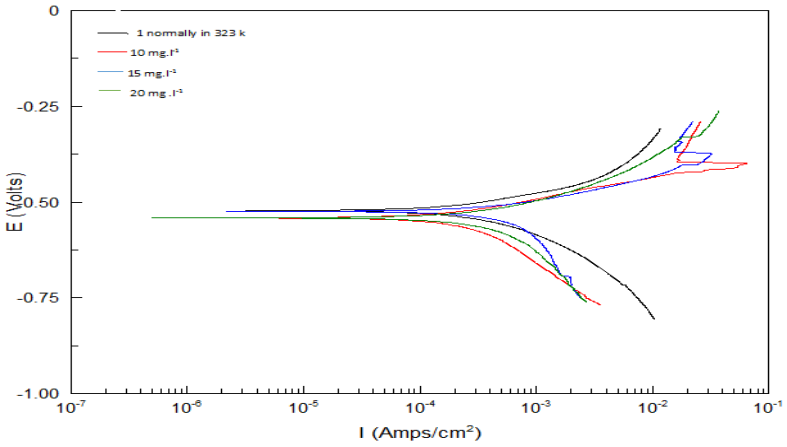

Figure 4a. Tafel plots for carbon steel (C1010) in 1M HCl with MEIG (10–20 ppm) at 323 K. (c)

The relationship between the corrosion rate of carbon steel immersed in an acidic medium (0.1 M HCl) and different concentrations at different temperatures, as shown in figure 4.

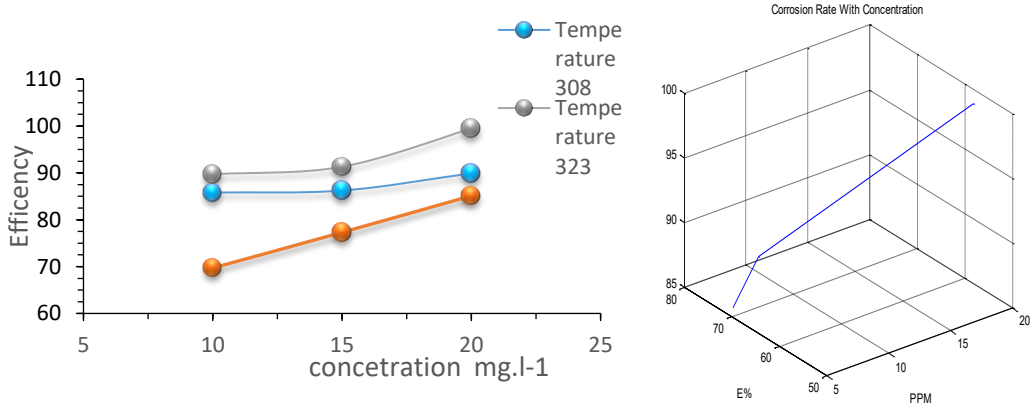

Figure 4. Corrosion rate of carbon steel (C1010) in 0.1M HCl with MEIG (5–20 ppm) at 298–328 K .b Corrosion rate of carbon steel (C1010) in 0.1M HCl with MEIG (5–20 ppm) at 298–328 K by MATLAB

4.4. The Effect of Inhibitor's Concentrations, Temperatures and Structures on the Corrosion Rate for Carbon Steel (C1010). The kinetic of Corrosion Reaction on the Carbon Steel Alloy

In order to study the effect of temperature on the activation energy value, the thermodynamic parameters of activation, such as ΔG*, ΔH* and ΔS*, were calculated from the Arrhenius equation. The activation energy value was calculated from Arrhenius to examine the effect of temperature Equation 3.

$$lnCR = lnA - Ea/RT \quad (3)$$

Where:

Ea = activation energy (KJ/ mol), CR = corrosion rate (mpy), R= molar of the gas constant (8.3143 $J.K^{-1}.mol^{-1}$), T = temperature (k), A = frequency factor inhibitors.

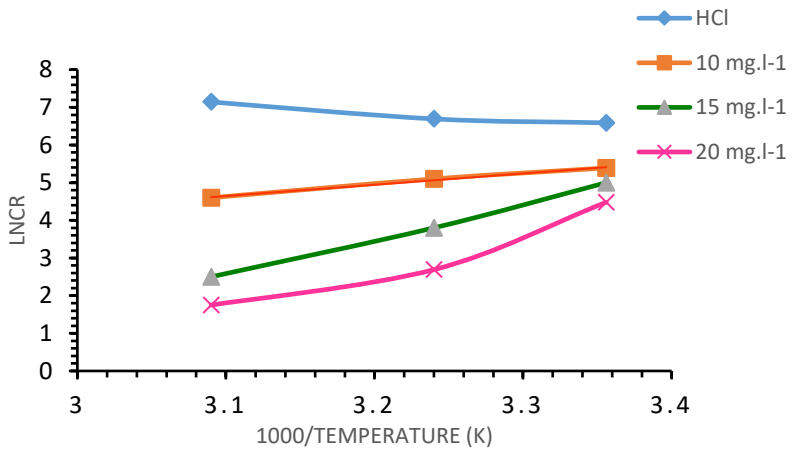

Figure 5. Energy activation for the corrosion reaction of carbon steel alloy (C1010) with and without the green inhibitor for methanolic extraction.

The activation energy was then determined when the slope of each graph in the graph above was equal to (-Ea/R). In addition, the following equation is plotted to determine additional kinetic parameters, such as, the entropy of activation (ΔS*), the enthalpy of activation (ΔH*) and the Gibbs free energy of activation (ΔG) were calculated by the plotting of the following Equation 4.

$$\frac{lnCR}{T} = \left(\frac{RT}{Nh}\right) \ln\left(\frac{\Delta S*}{R}\right) - \frac{\Delta H}{RT} \quad (4)$$

Where: N = Avogadro's number (6.022 × 1023 mol-1)

h = plank's constant (6.62 x 10-34 J.s)

Thus, the plotting of ln (CR/T) against (1/T) k-1 result the slope of (-ΔH*) and

It is possible to determine (ΔS*) from the intercept. Can be calculated. The plotting of equation are shown below in Figures.

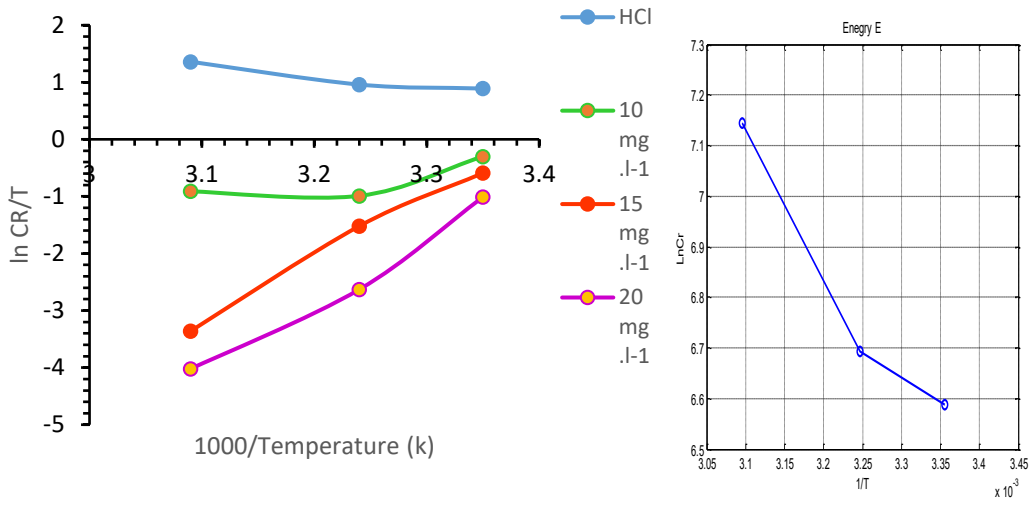

Figure 6. Calculation of the ΔS* and ΔH*for the corrosion reaction of the carbon steel alloy (C1010) in the presence and absence of green methanol extraction inhibitors Presence and absence of green methanol extraction inhibitors. B Calculation of the ΔS* and ΔH*for the corrosion reaction of the carbon steel alloy (C1010) in the presence and absence of green methanol extraction inhibitors Presence and absence of green methanol extraction inhibitors using MATLAB

Furthermore, the ΔG* was calculated according the following Equation 6.

$$\Delta G * = \Delta H * - T\Delta S * \quad (5)$$

All of the kinetic parameters were tabulated in Table 4

Table 4. Kinetic parameters Ea, ΔH*, ΔG* and ΔS* for the corrosion reaction of carbon steel (C1010) in presence and the absence of

constituents	Conc (ppm)	Ea* (kJ·mol⁻¹)	ΔH* (kJ·mol⁻¹)	ΔS* (J·K⁻¹·mol⁻¹)	ΔG*(kJ·mol⁻¹)		
					298	308	323
HCl (0.1N)	3650	17.7121	15.197	-24.4892	-22.495	-22.74	23.108
Methanolic extraction	10	-15.4674	17.971	-132.098	-21.393	-22.714	-24.696
	15	-77.844	83.921	-327.377	-13.636	-16.910	-21.821
	20	-83.7386	92.584	-934.572	-18.591	-19.526	-20.928

Where: Ea = activation energy; ΔH* = enthalpy of activation; ΔS* = entropy of activation; ΔG* = Gibbs free energy of activation.

From Table 4 above, the activation energy for the corrosion reaction of the alloy (C1010) in the presence of in the presence and absence of green methanol extraction inhibitors in this study is greater than in the absence of the specific inhibitor, which means that the energy barrier increases in the presence of the specific inhibitor compared to the absence of the inhibitor.

The enthalpy of activation (ΔH*) values are positive, indicating an endothermic behavior for the corrosion reaction. This holds true whether the inhibitors are present or absent. The endothermic nature of the corrosion reaction is enhanced in the presence of certain inhibitors, leading to an increase in corrosion reaction as temperature rises. The activation entropy (ΔS*) values are negative for all inhibitors, and they increase in the presence of each inhibitor as the corrosion species attempt to form an activated complex with the inhibitor molecules to create a protective film. This indicates a disordering process from reactant to activated complex. The activation free energy (ΔG*) include show that the corrosion reaction of the alloy is simultaneous at temperatures between 298-328 K in the absence of inhibitors. However, in the presence of any of the inhibitors, the values become positive, making the corrosion reaction non-spontaneous. This results in a reduction of the corrosion reaction and makes it more difficult in the presence of the inhibitor. [29-30]

4.5. The Studying of The Adsorption Reaction of The Inhibitor on the Carbon Steel Alloy's Surface.

Inhibitor on the surface of carbon steel alloy. Important details about the interaction between the inhibitor and the surface of carbon steel alloy are provided by the adsorption lines. In this study, the most suitable for all the studied inhibitors the Langmuir adsorption isotherm was found to be[31]. Various isotherms such as Timken, Freundlich, and Langmuir were used to analyze the organic compound adsorption. The Langmuir isotherm was selected as the best model due to its high correlation coefficient (R2) value close to one. The following formula was used to determine the Langmuir isotherm Equation 6. [32]

$$\frac{\theta}{1-\theta} = Kads\ C \tag{6}$$

The coverage surface (θ) for different concentrations inhibitor is determined using the adsorptive equilibrium constant (Kads) and inhibitor concentration (C). The Langmuir isotherms for various concentrations of an organic compound in 1M HCl at different temperatures are illustrated in Figures7.

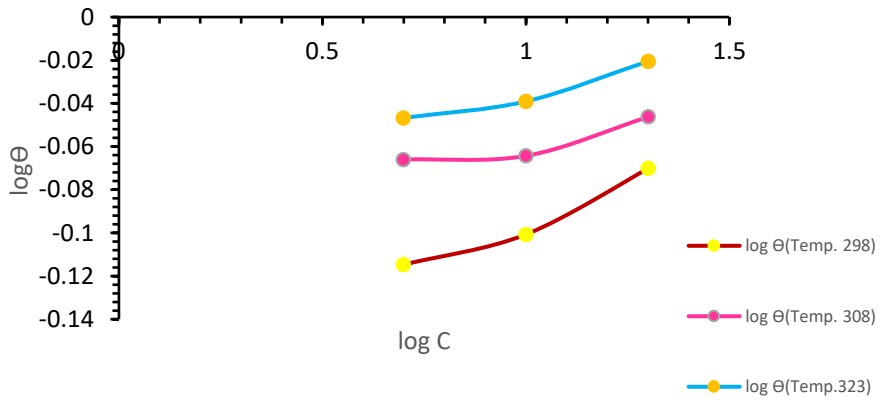

Figure 7. Langmuir s adsorption isotherm plots for the adsorption of (10-20) ppm on the surface of carbon steel surface against the corrosive environment of HCl at 298k. Inhibitors can be adsorbed through physisorption or chemisorption.

Physisorption includes weak interactions between organic ions or dipoles and the metal surface, while chemisorption involves sharing or charge transfer to form coordinated bonds. To calculate thermodynamic functions like free energy (ΔG°), enthalpy (ΔH°ads), and entropy (ΔS°ads) of adsorption, the equilibrium constant (K°ads) from Langmuir's adsorption isotherms for all inhibitors must be determined. The ΔG°ads can then be calculated using the Equation 7 below[33].

$$\Delta G°ads = RTln(55.5)Kads \tag{7}$$

Where, R is the gas constant, T is the experiment absolute temperature, and the constant value of 55.5 is the concentration of water in a solution in mol/L. The enthalpy of the adsorption ΔH° values for the inhibitors are calculated according the following Equation 8.

$$\frac{\Delta G°}{T} = \frac{\Delta H°}{T} + K \tag{8}$$

Thus, the variation of (ΔG°)/Ta opposite $1/T_{ads}$ to straight line with slope equal to ΔH° below shows the plotting of the above relationship.

The results also showed that the extract's inhibitory efficacy rises as the concentration of the inhibitor does, which may be related to the phytochemical components in the extract adsorbing onto the surface.[34, 35]

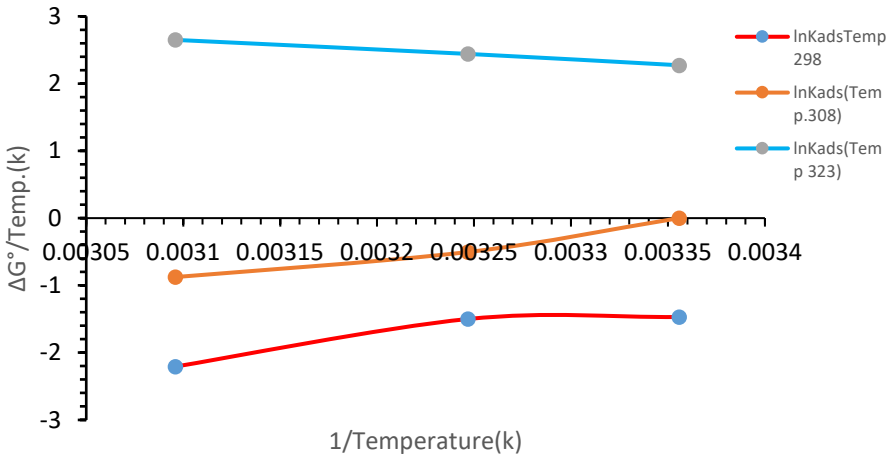

Figure 8. The calculation of ΔH°ads for the adsorption of corrosion on the carbon steel alloy's surface (C1010) at 298 k.

5. Conclusion

In this study, the methanolic extract of Inula graveolens L. (MEIG) demonstrated remarkable dual functionality as both an effective antioxidant and a highly efficient corrosion inhibitor for carbon steel in 1 M HCl solution. The antioxidant assays confirmed significant activity, with inhibition efficiencies reaching 73.9% for DPPH and 83% for β-carotene bleaching.

Electrochemical analysis using the Tafel polarization method revealed that MEIG provides excellent corrosion protection, achieving a maximum inhibition efficiency of 99.5% at 323 K. The inhibition performance was found to be dependent on both temperature and inhibitor concentration.

Thermodynamic and kinetic analyses indicated that the corrosion process in the presence of MEIG is endothermic and less spontaneous, with increased activation energy. Adsorption studies confirmed that MEIG molecules are predominantly physically adsorbed onto the carbon steel surface, following the Langmuir adsorption isotherm. The decrease in inhibition efficiency at higher temperatures was attributed to the weakening of adsorption and increased desorption processes.

The corrosion protection mechanism is mainly associated with the formation of a protective adsorbed layer that blocks active sites on the metal surface. Furthermore, MATLAB-based modeling provided additional support for the experimental findings and enhanced data interpretation. Overall, MEIG can be considered a promising, eco-friendly, and cost-effective candidate for industrial applications requiring both antioxidant and corrosion inhibition properties. Green corrosion inhibitors derived from plants offer a wide range of options, with many showing potential as effective and practical solutions for corrosion prevention. plant extract can be optimized to improve its antioxidant properties good antioxidant. The plant, especially the methanolic extract, showed very good properties and effectiveness as an antioxidant and an environmentally friendly corrosion inhibitor. Many studies and applications can be conducted.

References

1. Oliveira, M. S.; Chaves, O. S.; Cordeiro, L. V.; Gomes, A. N. P.; Fernandes, D. A.; Teles, Y. C. F.; Silva, T. M. d.; Freire, K. R. L.; Lima, E. O.; Agra, M. d. F.; J. Braz. Chem. Soc. 2023, 34, 220.
2. Matos, T. S.; Marques, M. S.; Chaves, C. J.; Zandonadi, F. S.; Palma-Silva, C.; Sussulini, A.; J. Braz. Chem. Soc. 2023, 34, 1631.
3. Iordache, A. M.; Nechita, C.; Podea, P.; Șuvar, N. S.; Mesaroș, C.; Voica, C.; Bleiziffer, R.; Culea, M.; Plants 2023, 12, 2183.
4. Arias, A.; Feijoo, G.; Moreira, M. T.; Innovative Food Sci. Emerging Technol. 2022, 77, 102974.
5. Donatien, E. A.; Rokiat, T. H.; Danquah, O.; Sodeyama, S.; Gbango, K. R.; Rodrigue, K. A.; Amani, B.; Marlene, N. P.; Benjamin, Y.; Appl. Chem. Eng. 2024, 7, 22.

6. Chowdhury, M. A.; Ahmed, M. M. S.; Hossain, N.; Islam, M. A.; Islam, S.; Rana, M. M.; Results Eng. 2023, 17, 100996.
7. Zakeri, A.; Bahmani, E.; Aghdam, A. S. R.; Corros. Commun. 2022, 5, 25.
8. Xiang, Q.; He, J.; J. Mol. Liq. 2021, 325, 115218.
9. Zahraa A. J; Falah K. M.;. Applied Chemical Engineering, 2025.8,3, ACE-5735. https://doi.org/10.59429/ace.v8i3.5735
10. Wang, Q.; Tan, B.; Bao, H.; Xie, Y.; Mou, Y.; Li, P.; Chen, D.; Shi, Y.; Li, X.; Yang, W.; Bioelectrochemistry 2019, 128, 49.
11. Fouda, A.; Gadow, H.; Abd Elal, E.; El-Tantawy, M.; J. Bio-Tribo-Corros. 2021, 7, 102.
12. Hossain, N.; Islam, M. A.; Chowdhury, M. A.; Results Chem. 2023, 5, 100883.
13. Maaroufi, Z.; Azdem, D.; El Mourabit, Y.; Alsayer, I.; Mabrouki, J.; El Hajjaji, S.; Applied Chemical Engineering 2025, 8, 3, ACE-5719.
14. Marzorati, S.; Verotta, L.; Trasatti, S. P.; Molecules 2018, 24, 48.
15. Serejo, R. C.; Macedo, H. P.; Medeiros, R. L.; Melo, D. M.; Figueredo, G. P.; Oliveira, M. M.; Rangel, J. H.; J. Braz. Chem. Soc. 2024, 35, e20240097.
16. Thakur, A.; Assad, H.; Kaya, S.; Kumar, A.; Handbook of Biomolecules; Elsevier: London, UK, 2023, pp 591-618.
17. Eljazi, J. S.; Selmi, S.; Zarroug, Y.; Wesleti, I.; Aouini, B.; Jallouli, S.; Limam, F.; Int. J. Food Prop. 2018, 21, 2309.
18. Baliyan, S.; Mukherjee, R.; Priyadarshini, A.; Vibhuti, A.; Gupta, A.; Pandey, R. P.; Chang, C.-M.; Molecules 2022, 27, 1326.
19. Abdelouhab, K.; Guemmaz, T.; Karamać, M.; Kati, D. E.; Amarowicz, R.; Arrar, L.; J. Pharm. Biomed. Anal. 2023, 235, 115673.
20. Lei, Y.; Qiu, Z.; Tan, N.; Du, H.; Li, D.; Liu, J.; Liu, T.; Zhang, W.; Chang, X.; Prog. Org. Coat. 2020, 139, 105430.
21. Wang, D.; Kijkla, P.; Saleh, M. A.; Kumseranee, S.; Punpruk, S.; Gu, T.; J. Mater. Sci. Technol. 2022, 130, 193.
22. Gulcin, İ.; Alwasel, S. H.; Processes 2023, 11, 2248
23. Sirivibulkovit, K.; Nouanthavong, S.; Sameenoi, Y.; Anal. Sci. 2018, 34, 795.
24. Faili, N. T.; Burghal, K. S.; Baghdad Sci. J. 2024, 21, 2319.
25. Holla, B. R.; Mahesh, R.; Manjunath, H.; Anjanapura, V. R.; Heliyon 2024, 10.
26. Huang, W.; Tang, Z.; Liu, X.; Liu, L.; Zhong, H.; Yu, Y.; Chen, H.; Wang, C.; Jiang, Q.; Ye, Y.; J. Mater. Res. Technol. 2024, 32, 2149.
27. 24. Li, Y.; Chen, Y.; Wang, C.; Li, Y.; Wu, Y.; Progress in Organic Coatings 2025, 198, 108915.
28. Mahalakshmi, K.; Malaya J. Math 2020, S2, 2261.
29. Verma, D. K.; Kaya, S.; Ech-chihbi, E.; El-Hajjaji, F.; Phukan, M. M.; Alnashiri, H. M.; J. Mol. Liq. 2021, 329, 115531.
30. Oualdi, I.; Diass, K.; Azizi, S.-e.; Dalli, M.; Touzani, R.; Gseyra, N.; Yousfi, E. B.; Nat. Prod. Res. 2023, 37, 2003.
31. Jafari, H.; Ameri, E.; Vakili, M. H.; Berisha, A.; Materials Chemistry and Physics 2024, 311, 128499.
32. Damej, M.; Kaya, S.; Ibrahimi, B. E.; Lee, H.; Molhi, A.; Serdaroğlu, G.; Benmessaoud, M.; Ali, I.; Hajjaji, S. E.; Lgaz, H.; Surf. Interfaces 2021, 24, 101095.
33. Farag, A. A.; Toghan, A.; Results in Engineering 2025, 25, 104504.
34. Zinad, D.; Jawad, Q.; Hussain, M.; Mahal, A.; Mohamed, L.; Al-Amiery, A.; Int. J. Corros. Scale Inhib. 2020, 9, 134.
35. Zaidon, F. H.; Kassim, K.; Zaki, H. M.; Embong, Z.; Hashim, N. Z. N.; J. Mol. Liq. 2021, 329, 115553.